Comput Mech (2009) 44:757–763
DOI 10.1007/s00466-009-0411-6

ORIGINAL PAPER

Winkler plate bending problems by a truly boundary-only boundary particle method

Zhuojia Fu · Wen Chen · Wei Yang

Received: 17 February 2009 / Accepted: 12 July 2009 / Published online: 28 July 2009
© Springer-Verlag 2009

Abstract This paper makes the first attempt to use the boundary particle method (BPM) to solve the problems of Winkler plate under lateral loading. In this study, we find that the standard fundamental solution does not work well with the BPM. Instead we construct the modified singular fundamental solution, which satisfies the homogeneous governing equation of Winkler plate and is employed in the BPM to calculate the homogeneous solution. Unlike the other boundary discretization methods, the BPM does not require any inner nodes to evaluate the particular solution of inhomogeneous problems, since the method is a truly boundary-only meshfree technique by using the recursive composite multiple reciprocity technique. Our numerical experiments demonstrate efficiency and high accuracy of the BPM in the solution of Winkler plate bending problems.

Keywords Boundary particle method · Recursive composite multiple reciprocity method · Winkler plate · Modified fundamental solution · Boundary-only · Meshfree

1 Introduction

In recent decades, the meshfree boundary-type collocation methods, such as method of fundamental solution (MFS) [1–3], boundary knot method (BKM) [4], boundary collocation method (BCM) [5], regularized meshless method (RMM) [6,7] and boundary node method (BNM) [8,9], have attracted a lot of attention in the numerical solution of various partial differential equations. All the above-mentioned boundary methods can solve homogeneous problems with boundary-only discretization. However, these methods require inner nodes in conjunction with the other techniques to handle inhomogeneous problems, such as quasi-Monte-Carlo method [10] and dual reciprocity method (DRM) [11].

Since 1980s the dual reciprocity method (DRM) and the multiple reciprocity method (MRM) [12] have been emerging as the two most promising techniques to calculate inhomogeneous problems in conjunction with the boundary type methods [11–13]. The striking advantage of the MRM over the DRM is that it does not require using inner nodes at all for the particular solution. To take advantage of its truly boundary-only merit, Chen developed the MRM-based meshfree boundary particle method (BPM) [14]. The BPM is a meshfree, integration-free strategy and applying either high-order nonsingular general solutions or singular fundamental solutions [15,16] as the radial basis function. Unlike the method of fundamental solutions with the dual reciprocity method (MFS-DRM) [17–20], the BPM does not require any inner nodes for inhomogeneous problems. And the method also requires much less computational effort for the discretization than the MR-BEM [21].

On the other hand, the standard MRM is computationally expensive in the construction of the interpolation matrix and has limited feasibility for general inhomogeneous problems due to its use of high-order Laplacian operators in the annihilation process [12]. Chen and Jin presented the recursive composite multiple reciprocity method (RC-MRM) [22,23], which employs the high-order composite differential operators to vanish the inhomogeneous term of various types. The RC-MRM significantly expands the application territory of the BPM to a much wider variety of inhomogeneous

Z. Fu · W. Chen (✉) · W. Yang
Center for Numerical Simulation Software in Engineering and Sciences, Department of Engineering Mechanics, College of Civil Engineering, Hohai University, No.1 XiKang Road, 210098 Nanjing, Jiangsu, China
e-mail: chenwen@hhu.edu.cn

Z. Fu
e-mail: paul212063@hhu.edu.cn

problems. In addition, the RC-MRM includes a recursive algorithm to dramatically reduce the total computing cost.

Some popular meshfree methods, such as element free Galerkin (EFG) method [24], meshless local Petrov-Galerkin (MLPG) [25–28], local boundary integral equation (LBIE) method [29], have been successfully applied to plate problems. However, all these methods require numerical integration. In this study, we make the first attempt to investigate the feasibility of the integration-free and boundary-only BPM in the solution of the Winkler plate bending problems. In particular, we find that the standard fundamental solution does not work well with the BPM. Instead we construct the modified singular fundamental solution, which satisfies the homogeneous governing equation of Winkler plate and is employed in the BPM to calculate the homogeneous solution. The BPM solutions are compared with those of the Hermite collocation method [30] and the MFS-DRM.

The remaining part of this paper is organized as follows. Section 2 introduces the BPM based on RC-MRM through the discretization of Winkler plate bending problems, followed by the Sect. 3 to numerically examine the efficiency and utility of this new technique. Finally, Sect. 4 concludes this paper with some remarks and opening issues.

2 RC-MRM based BPM for Winkler plate

The deflection of Winkler plate under the lateral loading $q(x)$ is governed by the following equation

$$\left(\Delta^2 + \frac{k}{D}\right) w = \frac{q(x)}{D}, \quad x \in \Omega, \tag{1}$$

where w is the deflection of the middle surface of plate, k denotes the foundation stiffness, and $D = \frac{Eh^3}{12(1-\nu^2)}$ represents the flexural rigidity with Young's Modulus E and Poisson's ratio of elasticity ν, the thickness of the plate h.

The Winkler plate fundamental solution [31] and general solution [16] can be respectively written as

$$G_1(r) = \mathrm{kei}\left(\left(\frac{k}{D}\right)^{1/4} r\right), \tag{2}$$

$$G_2(r) = \mathrm{ber}\left(\left(\frac{k}{D}\right)^{1/4} r\right), \tag{3}$$

Which respectively satisfies the following representation

$$\left(\Delta^2 + \frac{k}{D}\right) G_1(r) = \delta(r), \tag{4}$$

$$\left(\Delta^2 + \frac{k}{D}\right) G_2(r) = 0, \tag{5}$$

where *kei* represents the modified Kelvin functions of the second kind, ber denotes the Kelvin functions of the first kind, and $r = \|x - s\|_2$ is the distance between the source point s and the boundary collocation point x, $\delta(r)$ Dirac delta function.

Unfortunately, we find that fundamental solution (2) and general solution (3) cannot work well with the BPM. This study constructs a modified Winkler plate fundamental solution by a linear combination of solutions (2) and Eq. (3).

To evaluate the particular solution, this study uses the RC-MRM to avoid the inner nodes. Unlike the original MRM, the RC-MRM annihilate the inhomogeneous term by using a composite differential operator which can be different from the original governing differential operator. It eliminates the inhomogeneous term $q(x)$ in Eq. (1) by iterative differentiations

$$L_m \ldots L_2 L_1 \{q(x)\} \cong 0, \tag{6}$$

where $L_1, L_2, \ldots, L_m$ are differential operators of the same or different kinds. Appendix displays fundamental solutions of some commonly-used differential operators [14–16]. According to Eq. (6), Eq. (1) can be transformed into the following high-order homogeneous problem:

$$\begin{cases} L_m \ldots L_2 L_1 \left(\Delta^2 + \frac{k}{D}\right) w = 0 & x \in \Omega \\ \qquad\qquad \vdots & \\ L_2 L_1 \left(\Delta^2 + \frac{k}{D}\right) w = L_2 L_1 \left(\frac{q(x)}{D}\right) & x \in \partial\Omega \\ L_1 \left(\Delta^2 + \frac{k}{D}\right) w = L_1 \left(\frac{q(x)}{D}\right) & x \in \partial\Omega \\ \left(\Delta^2 + \frac{k}{D}\right) w = \frac{q(x)}{D} & x \in \partial\Omega \end{cases}. \tag{7}$$

Now we see that the solution of the inhomogeneous Winkler plate Eq. (1) can be evaluated by high-order homogeneous solution of Eq. (7).

In conjunction with appropriate boundary conditions of Winkler plates, the homogeneous governing Eq. (7) can be simply solved by boundary discretization. At each boundary point, the two out of four boundary conditions, i.e., displacement condition w, normal slope condition θ_n, bending moment condition M_n, and effective shear force V_n, have to be satisfied. Below is a list of the frequently encountered boundary conditions:

(1) Clamped edge: $w = 0, \theta_n = 0$;
(2) Simply supported edge: $w = 0, M_n = 0$;
(3) Free edge: $M_n = 0, \mathrm{V}_n = 0$.

The above boundary conditions can be expressed in terms of the deflection w as follows.

Normal slope:

$$\theta_n = \frac{\partial w}{\partial n} = \frac{\partial w}{\partial x}\frac{dx}{dn} + \frac{\partial w}{\partial y}\frac{dy}{dn} = \frac{\partial w}{\partial x}\cos\alpha + \frac{\partial w}{\partial y}\sin\alpha, \tag{8}$$

Normal bending moment:

$$M_n = -D\left\{\nu\nabla^2 w + (1-\nu)\left(\cos^2\alpha\frac{\partial^2 w}{\partial x^2} + \sin^2\alpha\frac{\partial^2 w}{\partial y^2} + \sin 2\alpha\frac{\partial^2 w}{\partial x\partial y}\right)\right\}, \tag{9}$$

Normal effective shear:

$$V_n = -D\left\{\left(\cos\alpha\frac{\partial}{\partial x} + \sin\alpha\frac{\partial}{\partial y}\right)\nabla^2 w + (1-\nu)\left(-\sin\alpha\frac{\partial}{\partial x} + \cos\alpha\frac{\partial}{\partial y}\right) \times \left(\frac{1}{2}\sin 2\alpha\left(\frac{\partial^2 w}{\partial y^2} - \frac{\partial^2 w}{\partial x^2}\right) + \cos 2\alpha\frac{\partial^2 w}{\partial x\partial y}\right)\right\} \tag{10}$$

where $n = [\cos\alpha, \sin\alpha]$ is the unit outward normal vector.

To illustrate the BPM procedure in the solution of plate bending problems, we consider the following Winkler plate.

Case 1 A simply-supported square plate with uniform loading q_0

$$\begin{cases} \left(\Delta^2 + \frac{k}{D}\right) w = \frac{q_0}{D} & x \in \Omega \\ w = 0 & x \in \partial\Omega \\ M_n = 0 & x \in \partial\Omega \end{cases}. \tag{11}$$

By implementing a Laplacian operation in the two sides of Eq. (11), the RC-MRM transforms the above inhomogeneous problem into the following high-order homogeneous problem.

$$\begin{cases} \Delta\left(\Delta^2 + \frac{k}{D}\right) w = 0, & x \in \Omega \\ \left(\Delta^2 + \frac{k}{D}\right) w = \frac{q_0}{D} & x \in \partial\Omega \\ w = 0 & x \in \partial\Omega \\ M_n = 0 & x \in \partial\Omega \end{cases}, \tag{12}$$

In general, the solution of Eq. (11) is equal to that of Eq. (12). Hence the deflection w can be approximated as follow

$$w(x, s_i) = \sum_{i=1}^{N}\alpha_i G_\Delta(x, s_i) + \sum_{i=1}^{N}\alpha_{N+i} G_1(x, s_i) + \sum_{i=1}^{N}\alpha_{2N+i} G_2(x, s_i), \tag{13}$$

where N represents the number of boundary points which are used in the BPM calculation, α_i is the unknown coefficients, and $G_\Delta(r) = \frac{1}{2\pi}\ln r$ the fundamental solution of Laplace equation. By substituting the above approximate expression (13) into Eq. (12), the unknown coefficients α_i can be obtained by solving the corresponding $3N$ linear equations.

$$A\alpha = b \tag{14}$$

where α is composed of the unknown coefficients α_j, $j = 1, 2, \ldots, 3N$.

$$A = \begin{bmatrix} \left(\Delta^2 + \frac{k}{D}\right) G_\Delta & 0 & 0 \\ G_\Delta & G_1 & G_2 \\ M_n(G_\Delta) & M_n(G_1) & M_n(G_2) \end{bmatrix}, \quad b = \begin{bmatrix} \frac{q_0}{D} \\ 0 \\ 0 \end{bmatrix}. \tag{15}$$

3 Numerical results and discussions

This section investigates the efficiency, accuracy, and convergence of the BPM on some Winkler plate bending problems, in comparison with the Hermite collocation method and the MFS-DRM.

3.1 Convergence rate and condition number of the RC-MRM based BPM

Unless otherwise specified, parameters in the tested plates are $E = 2.1\times10^{11}$, $h = 0.01$, $\nu = 0.3$, $q_0 = 10^6$, $k = \pi^4 D$. N denotes the number of boundary collocation points, Rerr represents the average relative error, Merr is the maximum absolute error, and Aerr denotes average absolute error, which are defined below

$$\mathrm{Rerr}(w) = \sqrt{\frac{1}{NT}\sum_{i=1}^{NT}\left|\frac{w(i) - w_e(i)}{w_e(i)}\right|^2}, \tag{16}$$

$$\mathrm{Merr}(w) = \max_{1\le i\le NT}|w(i) - w_e(i)|, \tag{17}$$

$$\mathrm{Aerr}(w) = \sqrt{\frac{1}{NT}\sum_{i=1}^{NT}|w(i) - w_e(i)|^2}, \tag{18}$$

where $w_e(i)$ and $w(i)$ are the analytical and numerical solutions evaluated at x_i, respectively, and NT is the total number of points in the domain and on the boundary which are used to measure the solution accuracy. Unless otherwise specified, NT is taken to be 2601 for plate bending problems. Please note that NT is much larger than N. The latter represents the number of points which are used in the BPM calculation. In this study, the fictitious boundary is chosen as a square with length $L = 2$, which is placed outside the unit square physical domain.

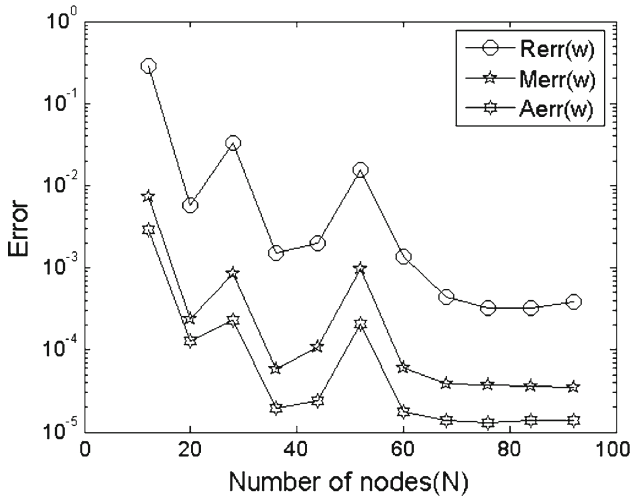

Fig. 1 The accuracy variation of case 1 against the number of interpolation knots

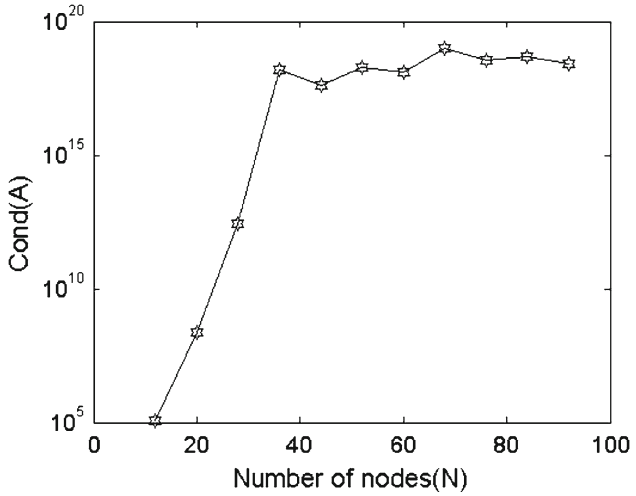

Fig. 2 The condition number of the interpolation matrices in case 1

We consider the simply-supported square plate in case 1, whose exact solution [32] is given by

$$w_e = \frac{16q_0}{\pi^6 D}\sum_{m=1}^{\infty}\sum_{n=1}^{\infty}\frac{\sin\frac{m\pi x}{a}\sin\frac{n\pi y}{b}}{mn\left[\left(\frac{m^2}{a^2}+\frac{n^2}{b^2}\right)^2+\frac{k}{\pi^4 D}\right]},$$
$$m=1,3,5,\ldots;\ n=1,3,5,\ldots \tag{19}$$

Figure 1 shows that the numerical accuracy with respect to the number of boundary collocation points N. It is observed that with increasing boundary points, numerical accuracy increases while heavy oscillation also appears largely thanks to a rapid increase of condition number of the BPM interpolation matrix as displayed in Fig. 2. Condition number *Cond* in Fig. 2 is defined as the ratio of the largest and smallest singular value. Such a ill-conditioned interpolation matrix problem is also found in the other boundary-type collocation techniques, such as the MFS [2,3] and the BKM [4]. There are several ways to handle this ill-conditioning problem, including the domain decomposition method [33], preconditioning technique based on approximate cardinal basis function, the fast multiple method [34] and regularization methods such as the truncated singular value decomposition (TSVD) [35].

This study will use the TSVD to mitigate the effect of bad conditioning in the BPM solution of the following other cases, and the generalized cross-validation (GCV) function choice criterion is employed to estimate an appropriate regularization parameter of the TSVD. Our computations use the MATLAB SVD code developed by Hansen [36].

Case 2 A clamped square plate with complex loading

$$\begin{cases}\left(\Delta^2+\frac{k}{D}\right)w=F(x,y) & x\in\Omega\\ w=0 & x\in\partial\Omega\\ \theta_n=0 & x\in\partial\Omega\end{cases}, \tag{20}$$

where the complex loading function

$$F(x,y)=\frac{q_0}{100D}\left(\left(64\pi^4+\frac{k}{D}\right)(\cos(2\pi x)-1)\times(\cos(2\pi y)-1)+48\pi^4(\cos(2\pi x)+\cos(2\pi y))-64\pi^4\right)$$

The exact solution is available as follows

$$w_e=\frac{q_0(\cos(2\pi x)-1)(\cos(2\pi y)-1)}{100D}, \tag{21}$$

By implementing composite operators, as shown in Eq. (23) below, in the two sides of Eq. (20), the RC-MRM transforms the above inhomogeneous equation into the following high-order homogeneous problem.

$$\begin{cases}\Delta\left(\Delta+\lambda_2^2\right)\left(\Delta+\lambda_1^2\right)\left(\Delta^2+k\right)w=0 & x\in\Omega\\ \left(\Delta+\lambda_2^2\right)\left(\Delta+\lambda_1^2\right)\left(\Delta^2+\frac{k}{D}\right)w & \\ \quad=\left(\Delta+\lambda_2^2\right)\left(\Delta+\lambda_1^2\right)F(x,y) & x\in\partial\Omega\\ \left(\Delta+\lambda_1^2\right)\left(\Delta^2+\frac{k}{D}\right)w=\left(\Delta+\lambda_1^2\right)F(x,y) & x\in\partial\Omega\\ \left(\Delta^2+\frac{k}{D}\right)w=F(x,y) & x\in\partial\Omega\\ w=0 & x\in\partial\Omega\\ \theta_n=0 & x\in\partial\Omega\end{cases}, \tag{22}$$

By using the RC-MRM, the inhomogeneous term $F(x,y)$ is eliminated by a composite differential operator $\Delta\left(\Delta+\lambda_2^2\right)\left(\Delta+\lambda_1^2\right)$, which includes Laplacian and Helmholtz operators. Namely,

$$\Delta\left(\Delta+\lambda_2^2\right)\left(\Delta+\lambda_1^2\right)F(x,y)=0, \tag{23}$$

where the parameter $\lambda_1=2\pi$, $\lambda_2=2\sqrt{2}\pi$.

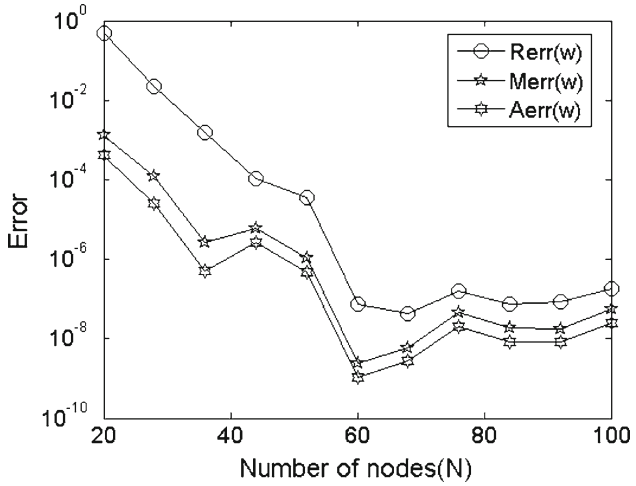

Fig. 3 The accuracy variation of case 2 against the number of interpolation knots

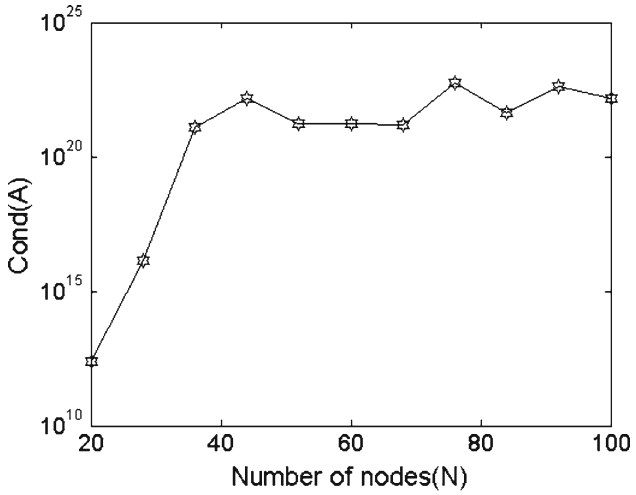

Fig. 4 The condition number of the interpolation matrices in case 2

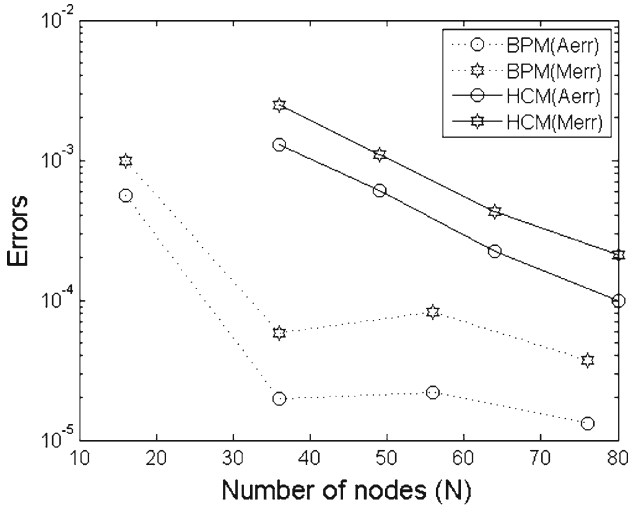

Fig. 5 The maximum and average absolute error curves of case 1 by using the boundary particle method and the Hermite collocation method

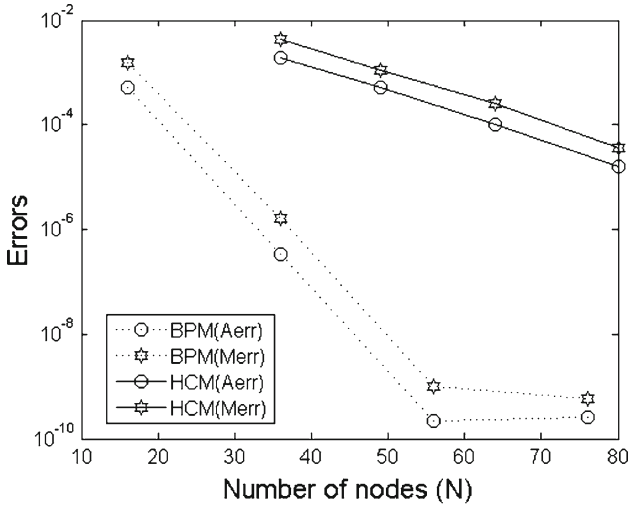

Fig. 6 The maximum and average absolute error curves of case 2 by using the boundary particle method and the Hermite collocation method

It is noted that the BPM cannot get the right solution in this case without using the TSVD technique. By implementing the TSVD to solve the ill-conditioning matrix system, Fig. 3 displays the numerical accuracy against the number of boundary nodes. It is observed that the relative errors are quickly reduced with increasing boundary nodes up to 60 nodes. Thereafter, we see all error curves become much more smooth and oscillatory, thanks to serious ill-conditioning of the interpolation matrix. Figure 4 shows the condition number of the interpolation matrix. In general, we note that the RC-MRM BPM performs better in case 2 than in case 1. The solution accuracy is very high and the convergence rate is fast. In this case, it is observed that the RC-MRM, using various differential operators to eliminate the lateral loading, is much more flexible and wider applicable than the original MRM only with Laplacian operators.

3.2 Comparisons with the Hermite collocation method and the MFS-DRM

This section compares the BPM with the other two radial basis function based meshfree methods, the Hermite collocation method (HCM) [30] and the MFS-DRM [20].

The MQ function with shape parameter 1 is chosen as the radial basis function in the present HCM. Note that N in the following figures represents the number of nodes. In particular, N in the HCM denotes the number of the uniform collocation points across the whole domain.

Figures 5 and 6 show the average and maximum absolute errors (Aerr and Merr) curves of cases 1 and 2 by using the BPM and the HCM. It is observed from Figs. 5 and 6 that the numerical accuracy of 16 nodes BPM solution is even better than that of 36 nodes HCM solution.

Table 1 The average relative error of case 1 by using the boundary particle method and the Hermite collocation method

Boundary particle method		Hermite collocation method	
Node number	Average relative error	Node number	Average relative error
36	1.90E-03	36	2.13E-02
56	2.90E-03	81	1.40E-03
76	3.29E-04	121	5.52E-04

Table 2 The average relative error of case 2 by using the boundary particle method and the Hermite collocation method

Boundary particle method		Hermite collocation method	
Node number	Average relative error	Node number	Average relative error
36	1.59E-04	36	6.79E-01
56	1.30E-06	81	5.20E-03
68	1.27E-06	121	1.18E-04

Tables 1 and 2 display the average relative error of cases 1 and 2 by using the BPM and the HCM. We can see that the BPM clearly outperforms the HCM in the numerical accuracy. It is also stressed that the BPM only requires the boundary discretization and has a particular edge over the domain discretization HCM for some real-world applications such as inverse problems, where only boundary data are usually available.

To compare the BPM with the MFS-DRM, we consider a reference case [20], namely, the deflection of a 2×2 clamped square plate. Its exact solution is as follow:

$$w_e = \sin\left(\frac{\pi x}{2}\right) \sin\left(\frac{\pi y}{2}\right). \tag{24}$$

The parameters of the plate are $D = 1$, $\nu = 0.33$, $k = \pi^4$ in terms of Eq. (1).

Tsai [20] concludes that the best average absolute errors of the MFS-DRM solution with 48, 64, 80 nodes are in range of $10^{-6} \sim 10^{-9}$ when fictitious boundary $L = 4$–8. In contrast, Fig. 7 illustrates the BPM and MFS-DRM convergence curves with the fictitious boundary $L = 8$. We can see from Fig. 7 that the numerical accuracy of 60 nodes BPM solution is comparable with that of 80 nodes MFS-DRM solution. Thus, the BPM uses fewer points than the MFS-DRM to obtain the numerical solutions of similar accuracy. It is noted that the BPM solutions do not invariably improved when the knots increase up to a certain number largely thanks to the round-off error effect of its ill-conditioned interpolation matrix. This is a common issue facing all global interpolation methods, such as Hermite collocation method [30].

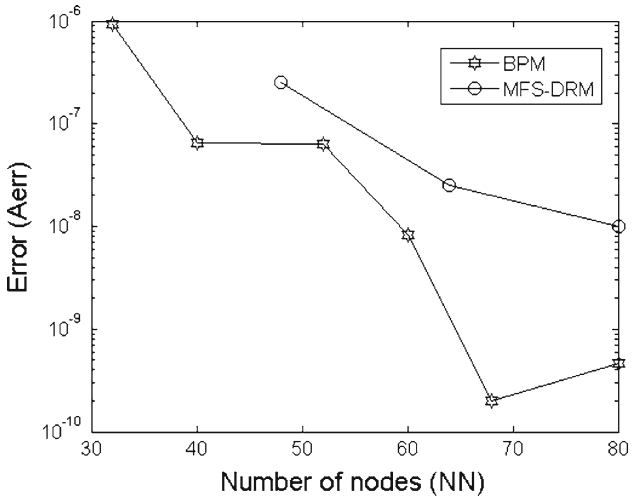

Fig. 7 The average absolute error curves of the BPM and the MFS-DRM

Unlike the MFS-DRM, the BPM does not require any additional interior points to evaluate the particular solution. Thus, the BPM is far more attractive than the MFS-DRM in the solution of inhomogeneous problems.

4 Conclusions

This paper extends the BPM based on RC-MRM to the Winkler plate under lateral loading. We find that the original fundamental solution [31] cannot work well with the BPM. And a modified fundamental solution of Winkler operator is constructed and is successfully employed with the BPM, as evidenced in the given numerical experiments. In some cases, owing to serious ill-conditioning of the interpolation matrix, the TSVD with GCV function choice criterion needs to be adopted to obtain accurate results. It is also stressed that the BPM solves the Winkler plate bending problems without using any inner collocation nodes, which is more attractive than the Hermite collocation method and the MFS-DRM in the solution of inverse and optimization problems, where only boundary data are usually accessible.

Acknowledgments We thank Prof. C.S. Chen for his very helpful comments and suggestions to improve academic quality and readability. The work described in this paper was supported by a research project funded by the National Natural Science Foundation of China (Project No. 10672051).

Appendix: Singular fundamental solutions

Table 3 is given for the readers to test the BPM. Here Δ denotes Laplacian, ∇ is the gradient operator, λ denotes wave number, $\mathbf{v}$ and $\mathbf{r}$, respectively, represent the velocity vector and distance vector, and r denotes the Euclidean distance. Y_0

Table 3 Singular fundamental solutions to commonly used differential operators

L	2D	3D
Δ	$-\frac{1}{2\pi}\ln r$	$\frac{1}{4\pi r}$
$\Delta+\lambda^2$	$\frac{1}{2\pi}Y_0(\lambda r)$	$\frac{\cos\lambda r}{4\pi r}$
$\Delta-\lambda^2$	$\frac{1}{2\pi}K_0(\lambda r)$	$\frac{e^{-\lambda r}}{4\pi r}$
$\Delta+\mathbf{v}\cdot\nabla-\lambda^2$	$\frac{1}{2\pi}K_0(\mu r)e^{-\frac{\mathbf{v}\cdot\mathbf{r}}{2}}$	$\frac{e^{-\mu r}}{4\pi r}e^{-\frac{\mathbf{v}\cdot\mathbf{r}}{2}}$

and K_0 are the Bessel and modified Bessel functions of the second kind of order zero, respectively.

References

1. Fairweather G, Karageorghis A (1998) The method of fundamental solutions for elliptic boundary value problems. Adv Comput Math 9:69–95
2. Chen CS, Cho HA, Golberg MA (2006) Some comments on the ill-conditioning of the method of fundamental solutions. Eng Anal Bound Elem 30:405–410
3. Wei T, Hon YC, Ling L (2007) Method of fundamental solutions with regularization techniques for Cauchy problems of elliptic operators. Eng Anal Bound Elem 31:163–175
4. Chen W, Tanaka M (2002) A meshless, exponential convergence, integration-free, and boundary-only RBF technique. Comput Math Appl 43:379–391
5. Chen JT, Chang MH, Chen KH, Lin SR (2002) The boundary collocation method with meshless concept for acoustic eigenanalysis of two-dimensional cavities using radial basis function. J Sound Vib 257:667–711
6. Young DL, Chen KH, Lee CW (2005) Novel meshfree method for solving the potential problems with arbitrary domain. J Comput Phys 209:290–321
7. Chen KH, Chen JT, Kao JH (2007) Regularized meshless method for antiplane shear problems with multiple inclusions. Int J Numer Meth Eng 73:1251–1273
8. Mukherjee YX, Mukherjee S (1997) The boundary node method for potential problems. Int J Numer Meth Eng 40:797–815
9. Zhang JM, Tanaka M, Matsumoto T (2004) Meshless analysis of potential problems in three dimensions with the hybrid boundary node method. Int J Numer Meth Eng 59:1147–1160
10. Chen CS, Golberg MA, Hon YC (1998) The method of fundamental solutions and quasi-Monte-Carlo method for diffusion equations. Int J Numer Meth Eng 43:1421–1435
11. Patridge PW, Brebbia CA, Wrobel LW (1992) The dual reciprocity boundary element method. Computational Mechanics Publication, Southampton
12. Nowak AJ, Neves AC (eds) (1994) The multiple reciprocity boundary element method. Computational Mechanics Publication, Southampton
13. Nowak AJ, Partridge PW (1992) Comparison of the dual reciprocity and the multiple reciprocity methods. Engng Anal Bound Elem 10:155–160
14. Chen W (2002) Meshfree boundary particle method applied to Helmholtz problems. Eng Anal Bound Elem 26:577–581
15. Itagaki M (1995) Higher order three-dimensional fundamental solutions to the Helmholtz and the modified Helmholtz equations. Eng Anal Bound Elem 15:289–293
16. Chen W, Shen ZJ, Yuan GW (2005) General solutions and fundamental solutions of varied orders to the vibrational thin, the Berger, and the Winkler plates. Eng Anal Bound Elem 29:699–702
17. De Medeiros GC, Partridge PW, Brandao JO (2004) The method of fundamental solutions with dual reciprocity for some problems in elasticity. Eng Anal Bound Elem 28:453–461
18. Chen CS, Brebbia CA, Power H (1999) Dual reciprocity method using compactly supported radial basis functions. Comm Num Meth Eng 15:137–150
19. Golberg MA, Chen CS, Bowman H, Power H (1998) Some comments on the use of radial basis functions in the dual reciprocity method. Comput Mech 21:141–148
20. Tsai CC (2008) The method of fundamental solutions with dual reciprocity for thin plates on winkler foundations with arbitrary loadings. J Mech 24:163–171
21. Sladek V, Sladek J (1996) Multiple reciprocity method in BEM formulations for solution of plate bending problems. Engng Anal Bound Elem 17:161–173
22. Chen W (2002) Distance function wavelets—Part III: "Exotic" transforms and series. Research report of Simula Research Laboratory, CoRR preprint
23. Chen W, Jin BT (2006) A truly boundary-only meshfree method for inhomogeneous problems The 2nd ICCES Special Symposium on Meshless Methods, Dubrovnik
24. Krysl P, Belytschko T (1995) Analysis of thin plates by the element-free Galerkin method. Comput Mech 17:26–35
25. Long SY, Atluri SN (2002) A meshless local Petrov Galerkin method for solving the bending problem of a thin plate. Comput Modeling Eng Sci 3:53–63
26. Sladek J, Sladek V, Zhang CH, Krivacek J, Wen PH (2006) Analysis of orthotropic thick plates by meshless local Petrov-Galerkin (MLPG) method. Int J Num Meth Eng 67:1830–1850
27. Sladek J, Sladek V, Hellmich CH, Eberhardsteiner J (2007) Analysis of thick functionally graded plates by local integral equation method. Commun Numer Methods Eng 23:733–754
28. Sladek J, Sladek V, Zhang CH (2008) Local integral equation method for viscoelastic Reissner-Mindlin plates. Comput Mech 41:759–768
29. Sladek J, Sladek V, Mang HA (2002) Meshless local boundary integral equation method for simply supported and clamped plates resting on elastic foundation. Comput Meth Appl Mech Eng 191:5943–5959
30. Leitão V (2001) A meshfree method for Kirchhoff plate bending problems. Int J Numer Meth Eng 52:1107–1130
31. Katsikadelis JT, Armenakas AE (1984) Plates on elastic foundation by BIE method. J Eng Mech 110:1086–1105
32. Timoshenko SP, Woinowsky-Krieger S (1959) Theory of plates and shells, 2nd edn. McGraw-Hill, New York
33. Kansa EJ, Hon YC (2000) Circumventing the ill-conditioning problem with multiquadric radial basis functions: applications to elliptic partial differential equations. Comput Math Appl 39:123–137
34. Beatson RK, Cherrie JB, Mouat CT (1999) Fast fitting of radial basis functions: methods based on preconditioned GMRES iteration. Adv Comput Math 11:253–270
35. Jin BT (2004) A meshless method for the Laplace and biharmonic equations subjected to noisy boundary data. CMES-Comput Model Eng Sci 6:253–261
36. Hansen PC (1994) Regularization tools: a Matlab package for analysis and solution of discrete ill-posed problems. Numer Algorithm 6:1–35